Supplementary Information

Decorating Nonpolar Units in Robust MOF for One-step Purification of C_2H_4 from $C_2H_2/C_2H_4/C_2H_6$

Qi Zhang, Rui Song, Lin Liu, Zheng-Bo Han**

4

College of Chemistry, Liaoning University, Shenyang 110036 P. R. China

**Corresponding authors E-mail: liulin@lnu.edu.cn; ceshzb@lnu.edu.cn.*

Supporting Information

1 Experimental procedures

1.1. Materials and instrumentation

All reagents were obtained commercially and utilized directly without additional purification. The morphologies of the prepared materials were examined with transmission electron microscopy (TEM) measurements (JEM-F200) and energy dispersive X-ray spectroscopy (EDX) was measured in 200 KV (EX-230 BUEX-37001). The chemical structures of relevant samples were examined by employing a Fourier transform infrared (FT-IR) spectrometer (Nicolet 5 DX). Powder X-ray diffraction (PXRD) was acquired with a diffractometer with Cu Kα radiation (Bruker D8 ADVANCE automated diffractometer, Germany). Raman spectroscopy was recorded with the Renishaw UV-1000 spectrometer. The N2 adsorption-desorption isotherms and BET surface area were characterized by a 3H-2000PS1 analyzer (Beishide Instrument Co., China).

N_2 (99.999%), C_2H_2 (99.9%), C_2H_4 (99.9%), C_2H_6 (99.9%), and He (99.999%) were purchased from Shenyang Shuntai Special Gas Co., Ltd. Ternary mixed gas ($C_2H_2/C_2H_4/C_2H_6$ 1/90/9) was purchased from Dalian Special Gases Co., Ltd.

1.2. Synthesis of MOF-808 and MOF-808-xFc

MOF-808 was synthesized with slight modifications from previous literature.[38] 1,3,5-benzene tricarboxylic acid (0.21 g) and $ZrOCl_2 \cdot 8H_2O$ (0.97 g) in a solution containing DMF and formic acid (60 mL 1:1) were dissolved in a 100 mL flask. The flask was heated in a 100 ℃ isothermal oven for 24 h. Then the white powder was collected by centrifugation (11000 rpm, 1 min), washed with DMF and acetone. Finally, MOF-808 was dried under a drying vacuum oven at 60 ℃.

MOF-808-xFc (x=1, 3, 6) was synthesized by a PSM method. Dissolving ferrocene carboxylic acid (1, 3, 6 eq to MOF-808) in DMF (60 mL) in a 100 mL bottle by ultrasonic until ferrocene carboxylic completely dissolved. Then MOF-808 (0.3 g) was suspended in the solution, and the suspension was heated at 100 ℃ oven for 24 h. Brown powder was collected by centrifugation (11,000 rpm, 1 min), washed with DMF and acetone. Finally, MOF-808-xFc was dried at ambient temperature.

1.3. Gas sorption experiment

Gas sorption isotherms were measured with BSD-660M analyzer (Beishide Instrument Co., China). The gas adsorption experiments of C_2H_2, C_2H_4 and C_2H_6 were conducted at 273 K and 298 K. Based on the gathered data, the adsorption isosteric heats were calculated by the Clausius - Clapeyron equation. All samples were heated under a high vacuum for solvent removal before conducting the test (100 ℃, 6 h).

1.4. Breakthrough measurements

The breakthrough experiment of C_2H_2/C_2H_4 and $C_2H_2/C_2H_4/C_2H_6$ were conducted on a fixed bed. The sample was packed in a stainless-steel column (length: 180 mm, inner diameter: 5 mm). Gas flows through the mass flow controller, the stainless-steel column and the gas chromatography (GC) with a TCD detector. MOF-808-xFc was

filled in the column and purged with He for 12 h at 80 ℃ to be activated. In continuous cycling experiments, samples were desorbed under heating conditions by He purging at 373 K for 120 min.

1.5. Isosteric heat of adsorption

Isosteric heat of adsorption (Q_{st}) is used to evaluate the adsorption affinity between the adsorbents and adsorbate molecules. The isosteric heat of adsorption at a given amount can be calculated by the Clausius-Clapeyron equation and it is defined as:

$$Q_{\mathrm{st}} = -RT^2\left(\frac{\partial lnp}{\partial T}\right)_{n_a}$$

where Q_{st} (kJ·mol^{-1}) is the isosteric heat of adsorption, P (kPa) is the pressure, T is the temperature, R is the gas constant, and n_a is the adsorption amount (mmol·g^{-1}). Integration of the equation gives.

$$\ln(\mathrm{p}) = \frac{Q_{st}}{RT} + \mathrm{C}$$

1.6. IAST calculations of adsorption selectivity

The adsorption selectivity were established by the Ideal Adsorbed Solution Theory (IAST) for C_2H_6/C_2H_4 = 50/50 (v/v), C_2H_6/C_2H_4 = 10/90 (v/v) and C_2H_2/C_2H_4 = 1/99 (v/v) binary mixtures. The adsorption selectivity, S_{ij}, is defined by the following equation:

$$S_{ij} = \frac{x_i/x_j}{y_i y_j}$$

where x_i and x_j are the equilibrated adsorption capacity of component i and j, respectively; and y_i and y_j are the molar fractions of component i and j in gas phase, respectively.

1.7. Grand Canonical Monte Carlo and simulation details

The GCMC calculation was performed to determine the adsorption sites distribution among two MOFs for all adsorbates. All the GCMC simulations were performed using the Forcite and Sorption modules of Materials Studio software (2019). The unit cell was constructed using the cif files of MOF-808 obtained from the reported by Yaghi et al.[1] According to the high similarity of PXRD patterns between MOF-808 series, built a crystal structure model for MOF-808-6Fc by substituting formic acid with ferrocene carboxylic acid based on the framework connection of MOF-808.

1.8. Density functional theory calculations

First-principles density functional theory (DFT) calculations were conducted using the Materials Studio's DMol3 and adsorption locator. For the framework, one quarter of the Zr6 cluster was extracted for DFT calculation. All calculations were performed

under the generalized gradient approximation (GGA) with Perdew-Burke-Ernzerhof (PBE). The structures of the synthesized materials were first optimized. The target gas molecules were then introduced to different locations of the channel pore. The static binding energy was calculated by the equation: $\Delta E_b = E(\text{gas}) + E(\text{adsorbent}) - E(\text{adsorbent + gas})$.

2 Supplementary figures

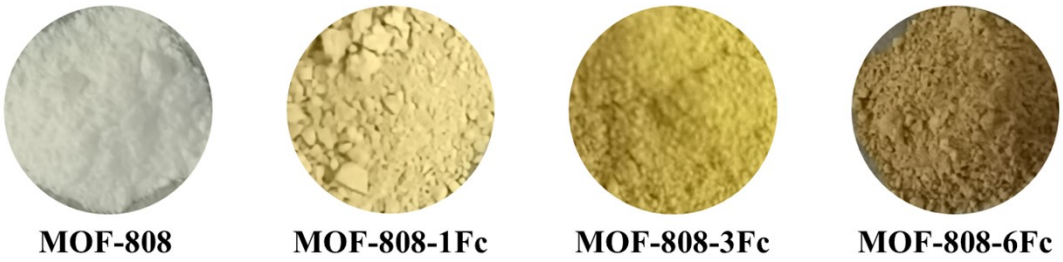

Fig. S1. Powder samples of MOF-808, MOF-808-1Fc, MOF-808-3Fc and MOF-808-6Fc.

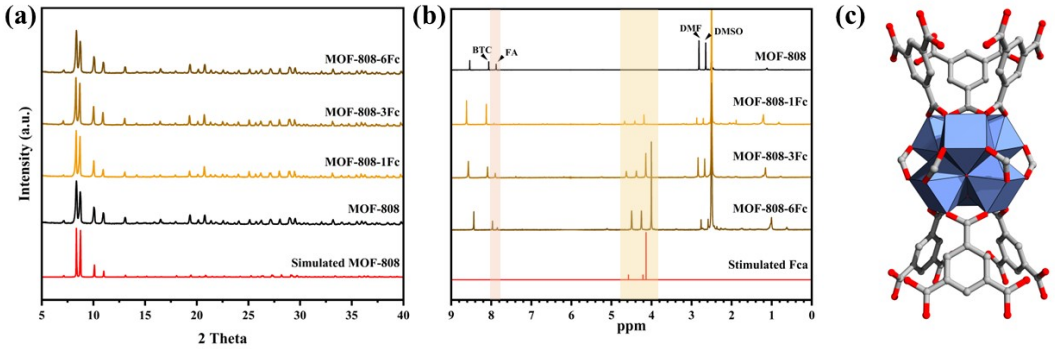

Fig. S2. a) PXRD patterns of MOF-808 and MOF-808-xFc; b) 1H NMR spectrum related to MOF-808 and MOF-808-xFc; c) the inorganic SBU of MOF-808.

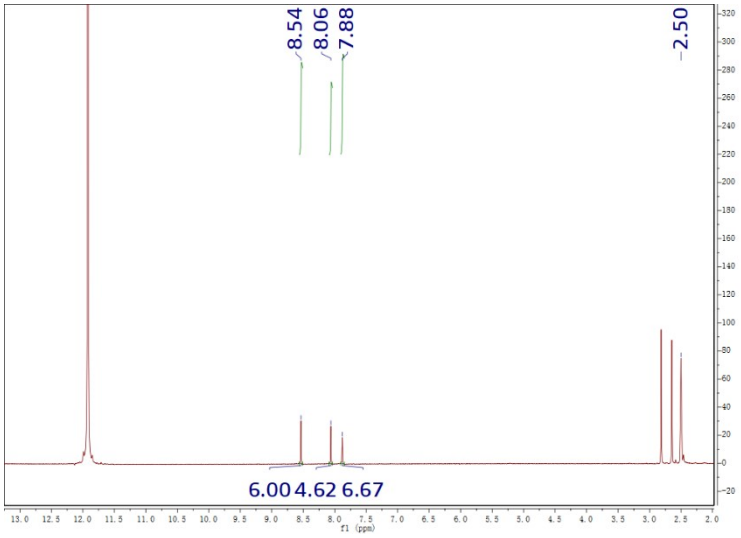

Fig. S3. Original ^{1}H-NMR spectra of MOF-808.

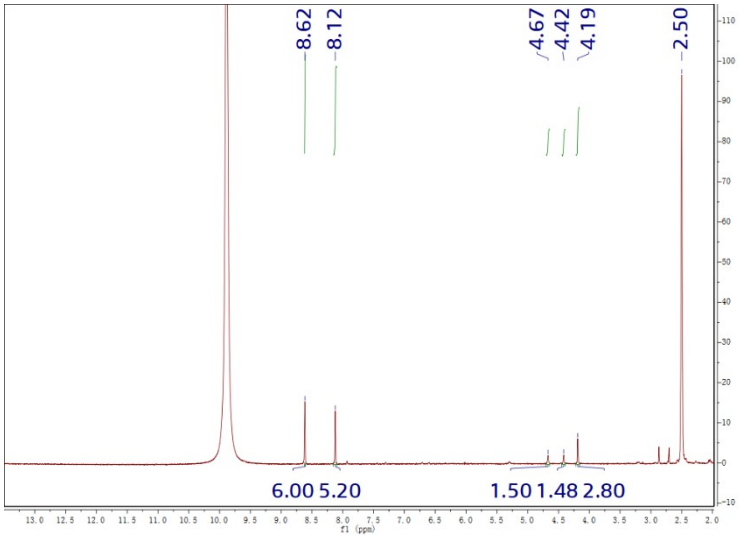

Fig. S4. Original ^{1}H-NMR spectra of MOF-808-1Fc.

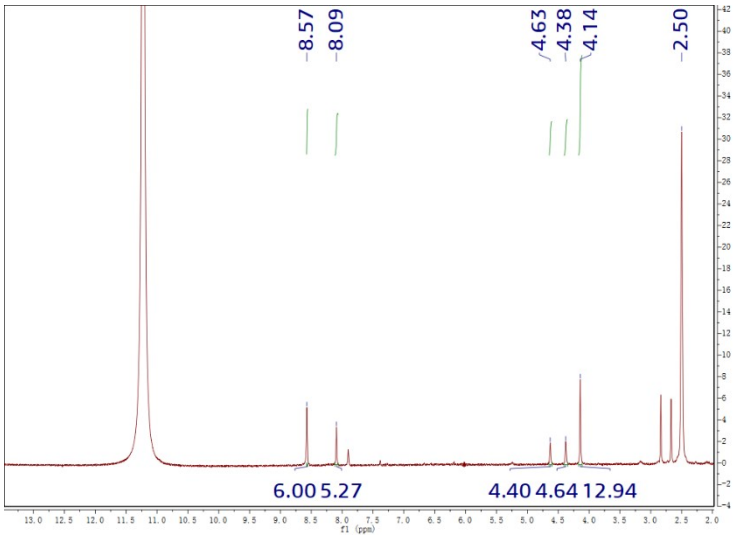

Fig. S5. Original ^{1}H-NMR spectra of MOF-808-3Fc.

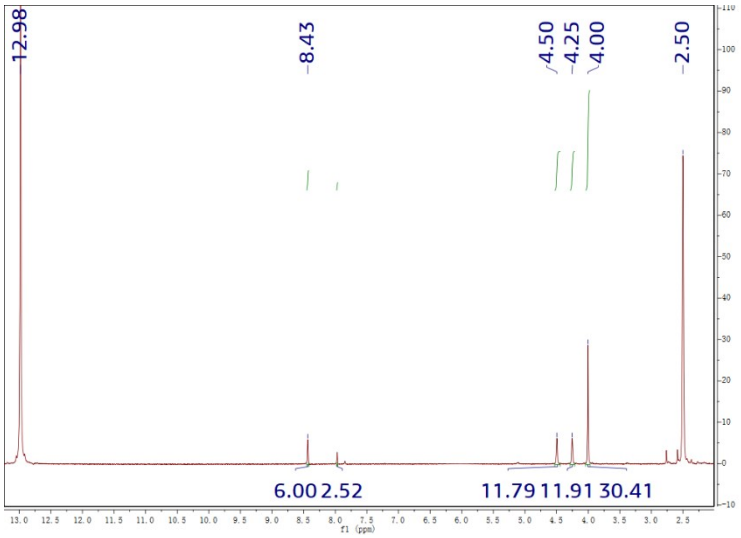

Fig. S6. Original ^{1}H-NMR spectra of MOF-808-6Fc.

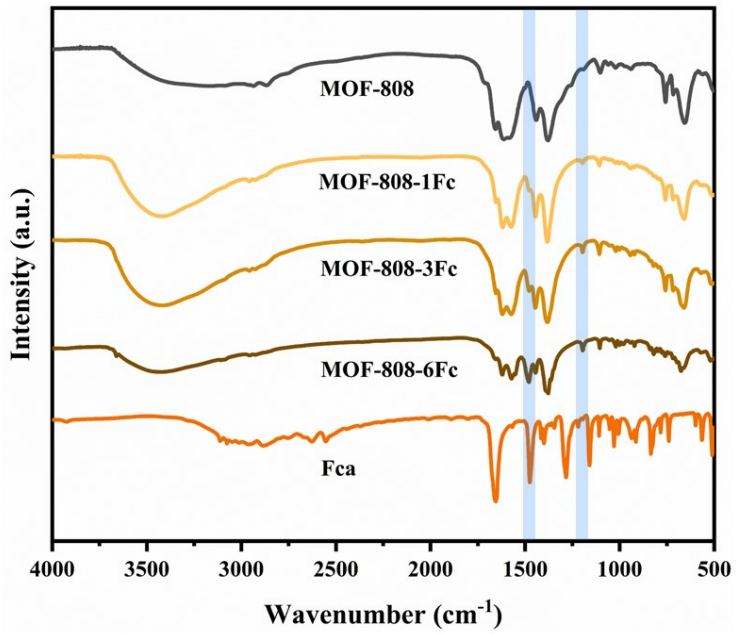

Fig. S7. FT-IR spectra of MOF-808 (black), MOF-808-1Fc (light brown), MOF-808-3Fc (brown), MOF-808-6Fc (dark brown), Fc (orange) and H_3BTC (Navy).

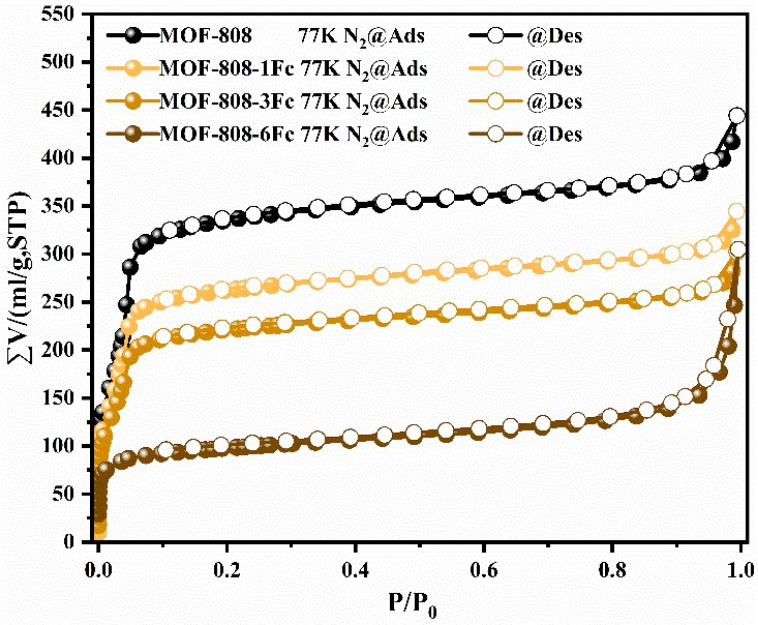

Fig. S8. Nitrogen adsorption isotherms of MOF-808, MOF-808-1Fc, MOF-808-3Fc and MOF-808-6Fc at 77 K.

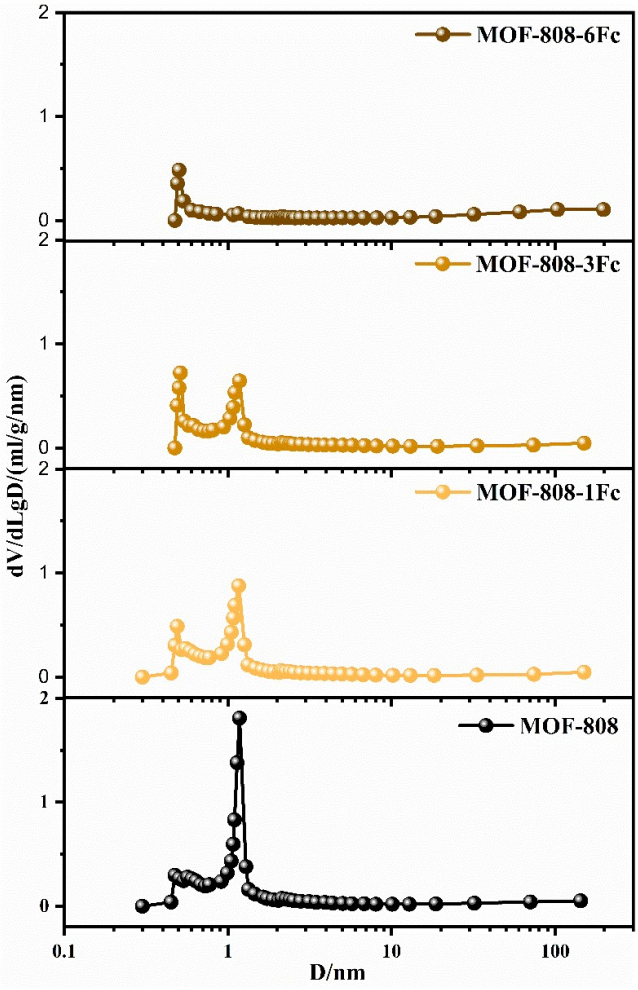

Fig. S9. Calculated pore size distribution calculated of MOF-808, MOF-808-1Fc, MOF-808-3Fc and MOF-808-6Fc by density functional theory.

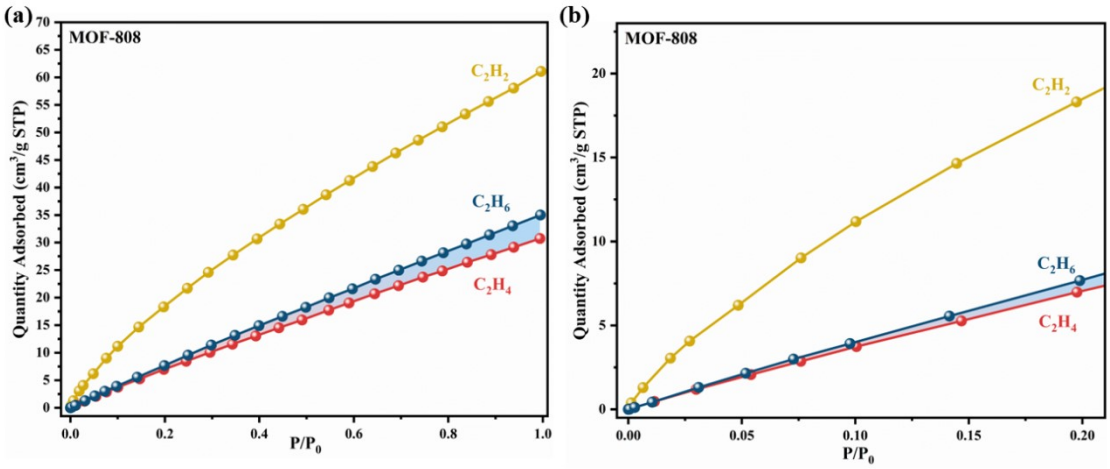

Fig. S10. Experimental adsorption of C_2H_2 (yellow), C_2H_4 (red) and C_2H_6 (blue) on MOF-808 at 273K (a) atmospheric pressure zone (b) low pressure zone.

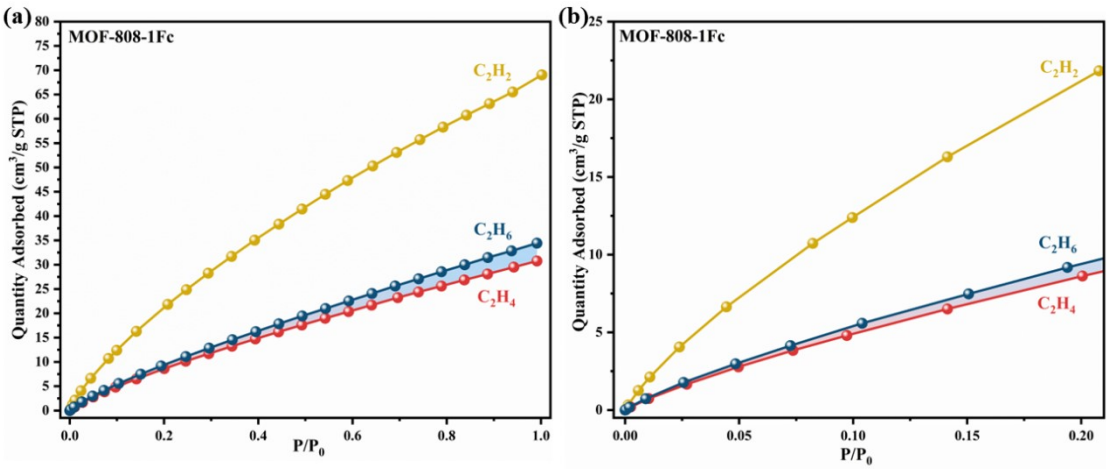

Fig. S11. Experimental adsorption of C_2H_2 (yellow), C_2H_4 (red) and C_2H_6 (blue) on MOF-808-1Fc at 273K (a) atmospheric pressure zone (b) low pressure zone.

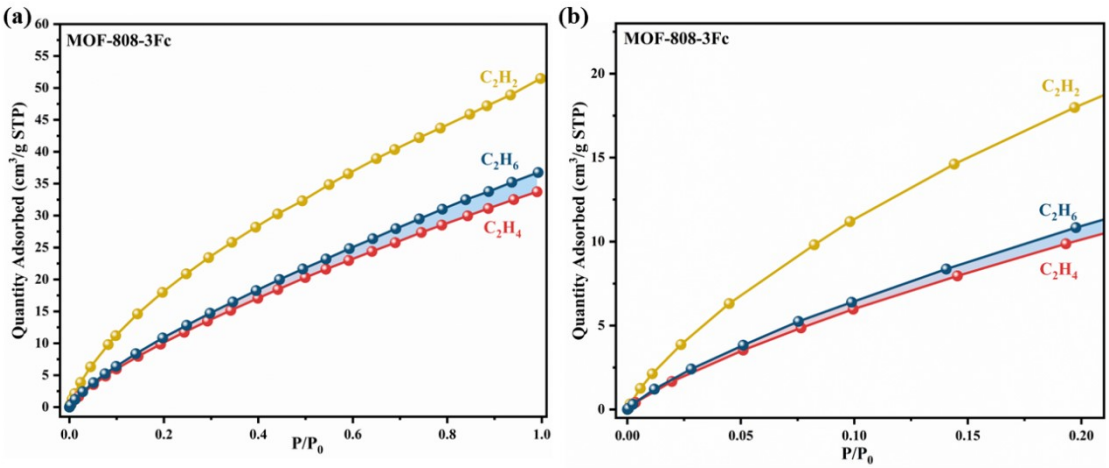

Fig. S12. Experimental adsorption of C_2H_2 (yellow), C_2H_4 (red) and C_2H_6 (blue) on MOF-808-3Fc at 273K (a) atmospheric pressure zone (b) low pressure zone.

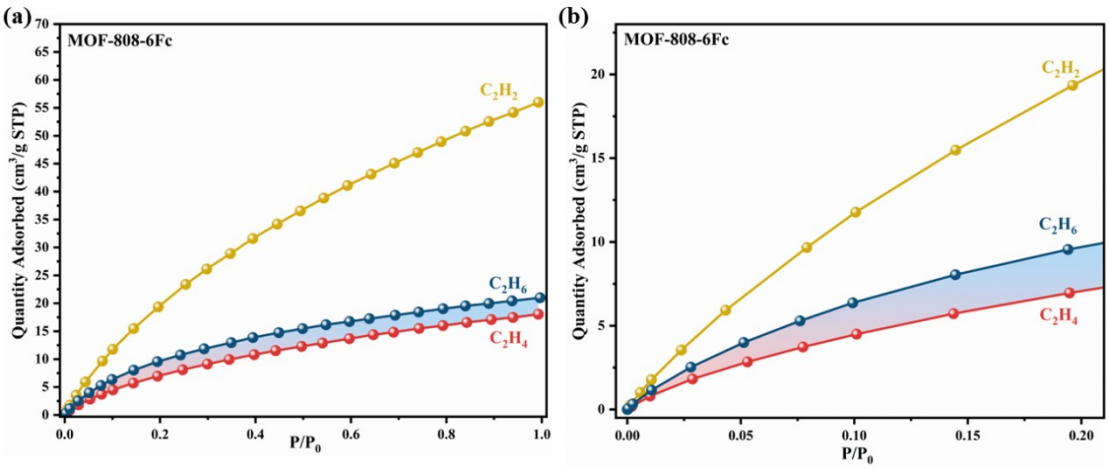

Fig. S13. Experimental adsorption of C_2H_2 (yellow), C_2H_4 (red) and C_2H_6 (blue) on MOF-808-6Fc at 273K (a) atmospheric pressure zone (b) low pressure zone.

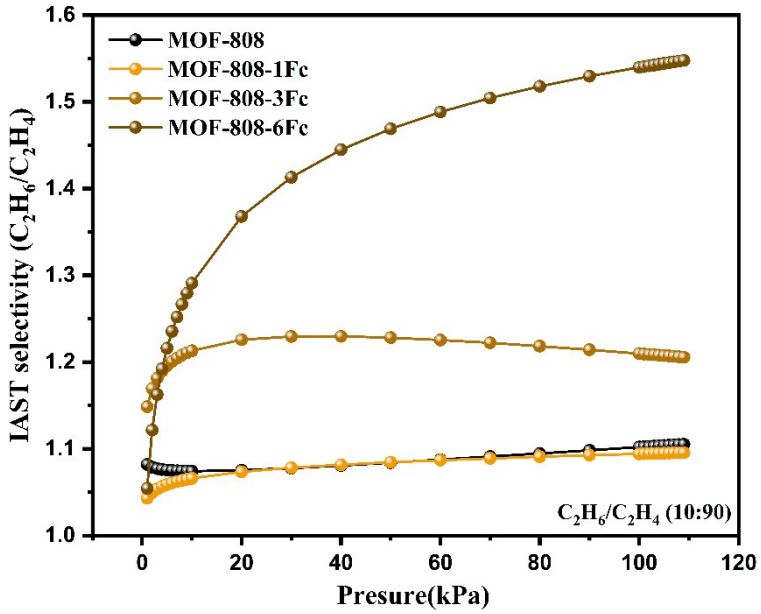

Fig. S14. IAST selectivity of MOF-808 and MOF-808-xFc for C_2H_6/ C_2H_4 (10/90) at 298 K

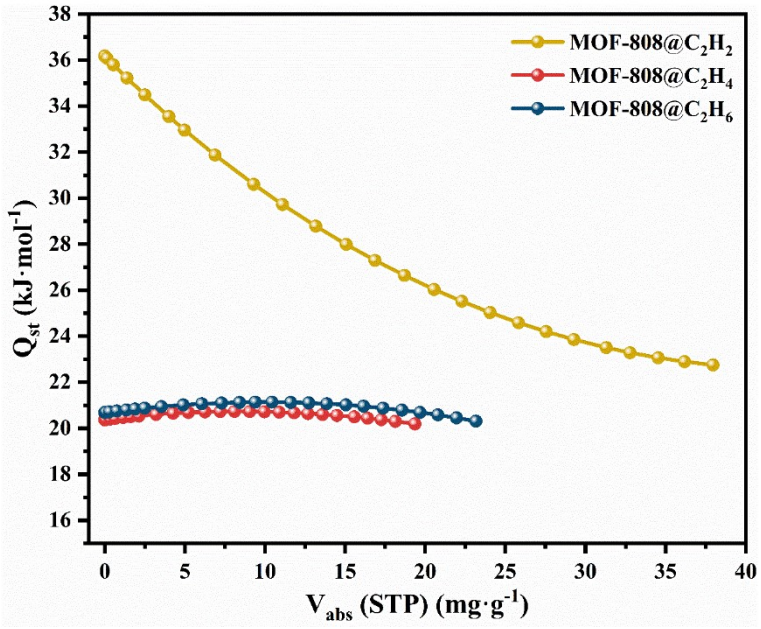

Fig. S15. The isosteric heats of adsorption (Q_{st}) of C_2H_2, C_2H_4 and C_2H_6 on MOF-808 calculated from its adsorption isotherms based on the Clausius-Clapeyron equation.

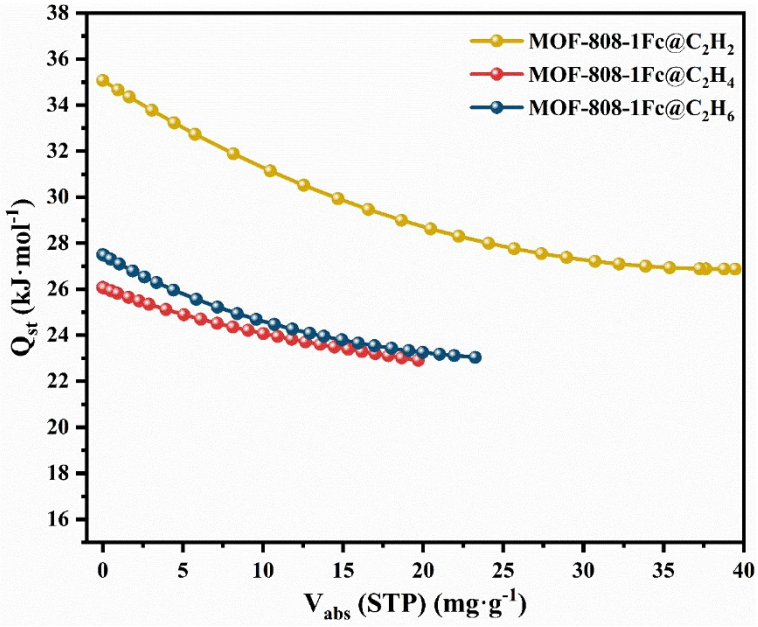

Fig. S16. The isosteric heats of adsorption (Q_{st}) of C_2H_2, C_2H_4 and C_2H_6 on MOF-808-1Fc calculated from its adsorption isotherms based on the Clausius-Clapeyron equation.

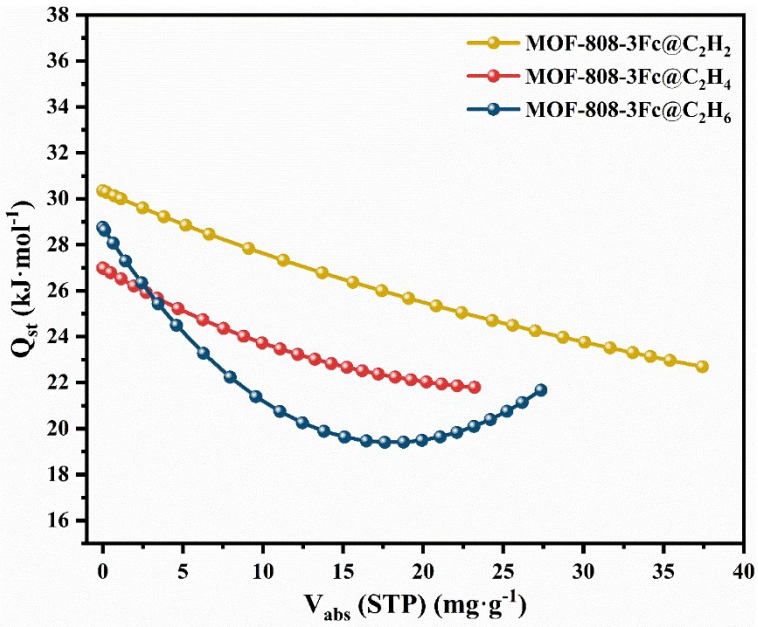

Fig. S17. The isosteric heats of adsorption (Q_{st}) of C_2H_2, C_2H_4 and C_2H_6 on MOF-808-3Fc calculated from its adsorption isotherms based on the Clausius-Clapeyron equation.

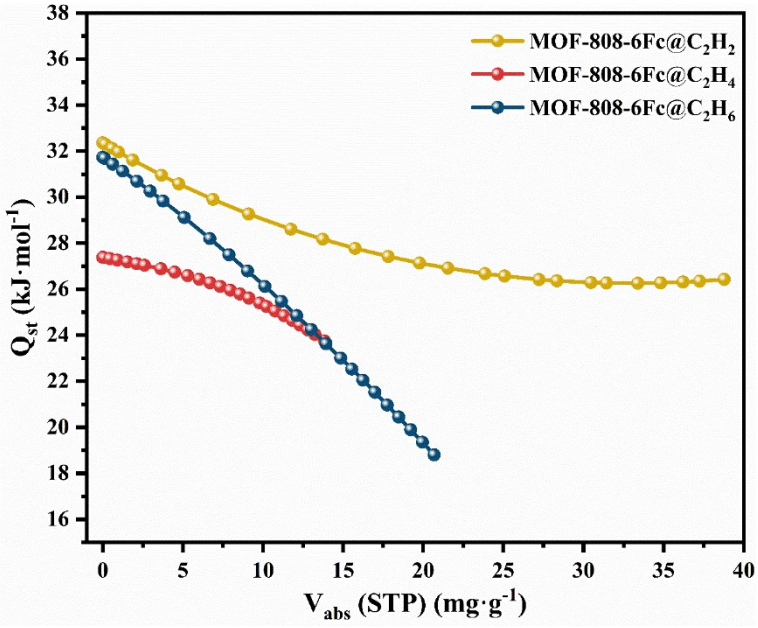

Fig. S18. The isosteric heats of adsorption (Q_{st}) of C_2H_2, C_2H_4 and C_2H_6 on MOF-808-6Fc calculated from its adsorption isotherms based on the Clausius-Clapeyron equation.

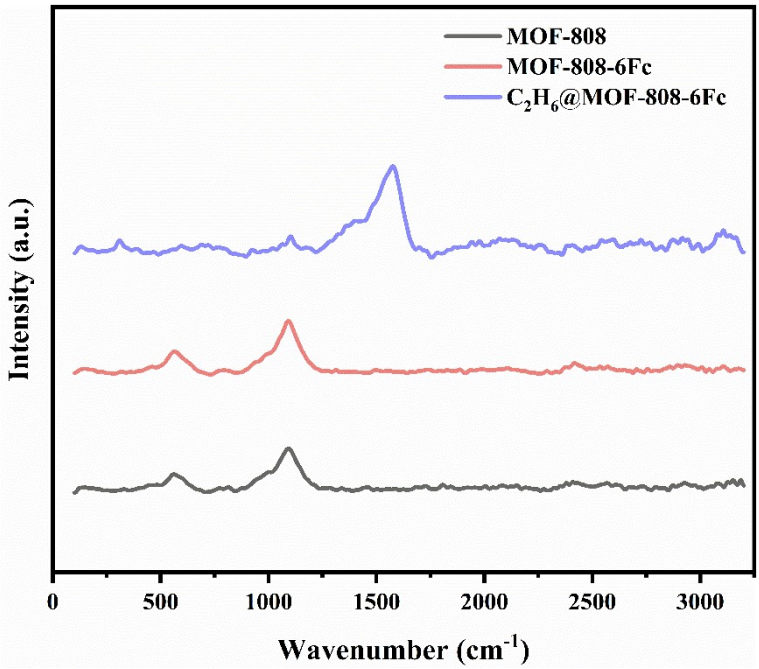

Fig. S19. Raman spectra of C_2H_6 absorbed by activated MOF-808 and MOF-808-6Fc.

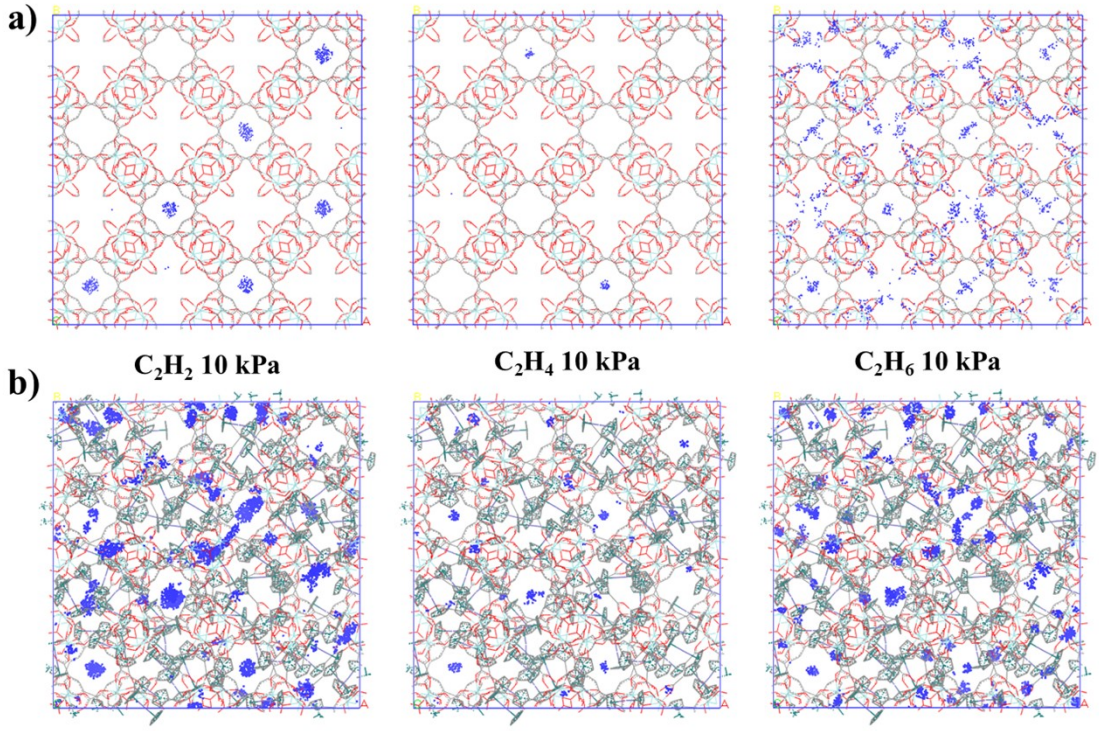

Fig. S20. The density distribution of C_2H_2, C_2H_4 and C_2H_6 on (a)MOF-808 and (b)MOF-808-6Fc at 10 kPa.

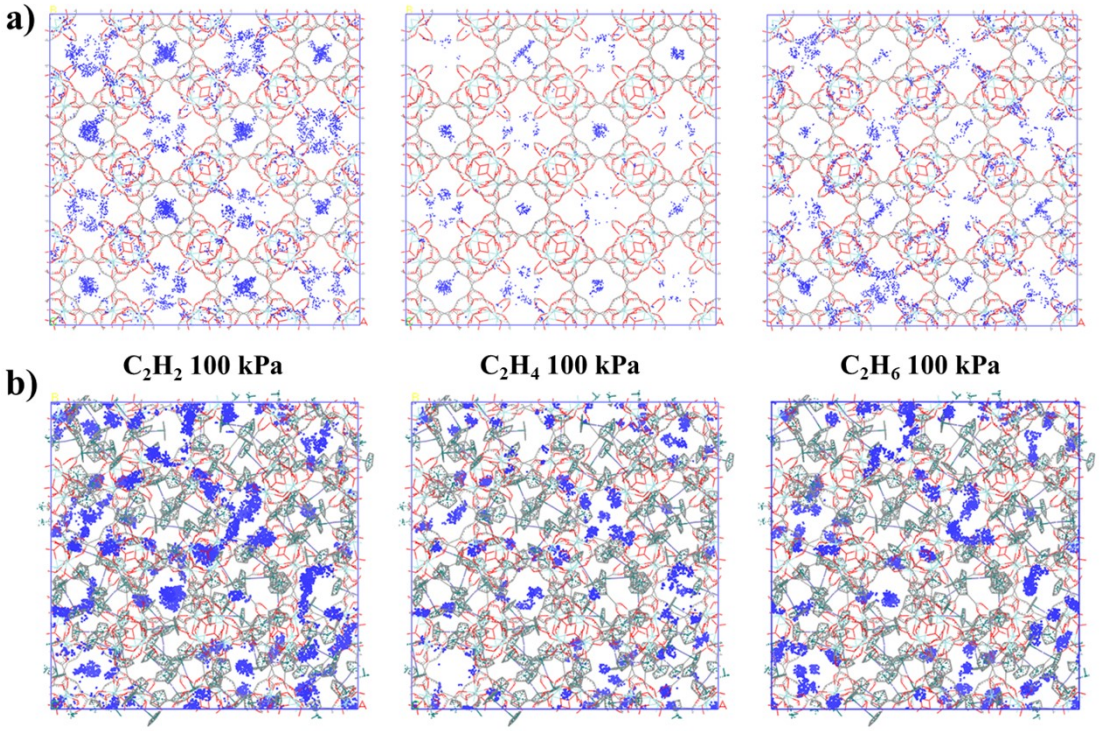

Fig. S21. The density distribution of C_2H_2, C_2H_4 and C_2H_6 on (a)MOF-808 and (b)MOF-808-6Fc at 100 kPa.

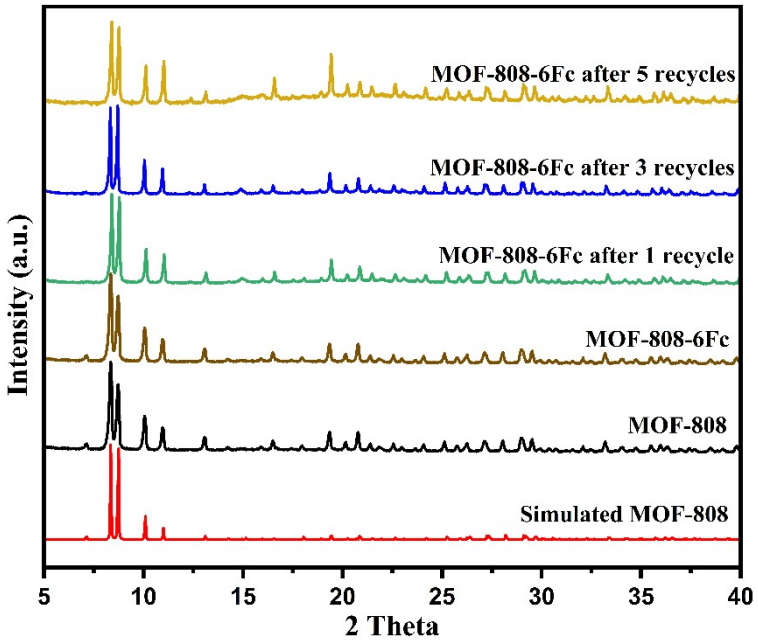

Fig. S22. PXRD results of MOF-808-6Fc after recycle tests.

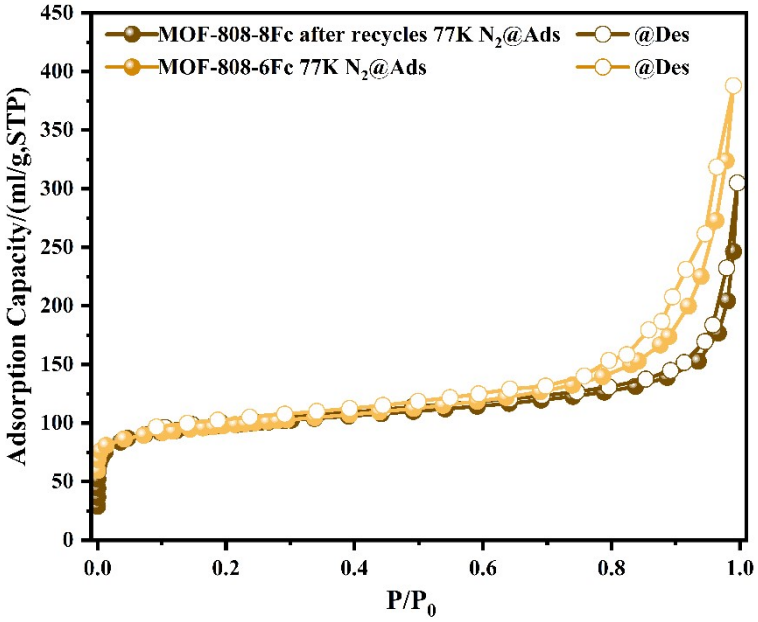

Fig. S23. 77K N_2 adsorption curve of MOF-808-6Fc after recycle tests.

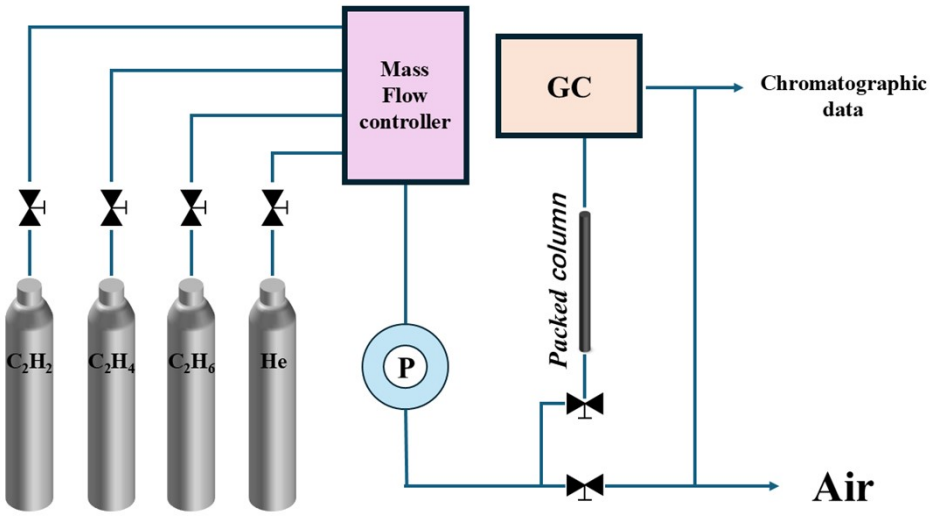

Fig. S24. Breakthrough experiments apparatus diagram.

3 Supplementary tables

Table S1. The physical properties of light hydrocarbons[5]

Adsorbate	B.P. (K)	Kinetic Diameter (Å)	Molecular size (Å)	Polarizability (10^{-25} cm^3)	Quadruple moment (10^{-26} esu cm^2)	Dipole moment (10^{-18} esu cm)
C_2H_2	188.4	3.2	3.3×3.3×5.7	33.3-39.3	7.2	0
C_2H_4	169.4	4.2	3.3×4.2×4.8	42.5	1.5	0
C_2H_6	184.5	4.4	3.8×4.1×4.8	44.3-44.7	0.65	0

Table S2. The adsorption capacity of samples at 100kPa.

Samples	C_2H_2 (cm^3/g)		C_2H_4 (cm^3/g)		C_2H_6 (cm^3/g)	
	273K	298K	273K	298K	273K	298K
MOF-808	61.08	36.27	30.73	15.49	35.00	17.29
MOF-808-1Fc	69.05	32.24	30.76	15.76	34.43	17.36
MOF-808-3Fc	51.48	34.01	33.73	18.56	36.75	20.42
MOF-808-6Fc	56.00	33.41	18.04	11.08	21.00	15.44

Table S3. The fitting parameters data by the Clausius-Clapeyron equation.

Samples	Adsorbates	a_0	a_1	a_2	a_3	a_4	a_5	b_0	b_1	b_2	R^2
MOF-808	C_2H_2	-4351.07	84.60	-1.46	0.01	-1.55 E^{-4}	6.65 E^{-7}	17.12	-0.24	2.90 E^{-3}	0.99995
	C_2H_4	-2450.20	-11.31	0.86	-0.02	5.10 E^{-4}	-4.57 E^{-6}	11.73	0.04	2.17 E^{-3}	0.99998
	C_2H_6	-2488.42	-10.28	0.44	6.58 E^{-3}	-1.34 E^{-4}	1.04 E^{-6}	11.39	0.09	-3.44 E^{-3}	0.99997
MOF-808-1Fc	C_2H_2	-4218.67	53.32	-0.79	1.94 E^{-3}	2.33 E^{-6}	-8.03 E^{-8}	16.63	-0.15	2.07 E^{-3}	0.99994
	C_2H_4	-3136.33	33.90	-1.39	0.05	-9.54 E^{-4}	7.50 E^{-6}	13.64	-0.04	2.89 E^{-4}	0.99999
	C_2H_6	-3308.26	49.08	-1.78	0.04	-7.31 E^{-4}	4.96 E^{-6}	14.05	-0.10	1.82 E^{-3}	0.99997
MOF-808-3Fc	C_2H_2	-3651.00	37.60	-0.54	0.01	-7.79 E^{-5}	3.09 E^{-7}	14.36	-0.07	4.08 E^{-4}	0.99997
	C_2H_4	-3246.55	50.58	-1.19	0.01	5.76 E^{-5}	-1.40 E^{-6}	13.80	-0.12	2.28 E^{-3}	0.99998
	C_2H_6	-3459.36	129.31	-3.99	0.02	-8.12 E^{-5}	-5.30 E^{-7}	15.53	-0.56	0.02	0.99990
MOF-808-6Fc	C_2H_2	-3892.72	50.48	-1.17	0.01	0.01	-1.86 E^{-4}	15.33	-0.13	2.14 E^{-3}	0.99999
	C_2H_4	-3293.62	14.82	-0.02	0.14	-4.93 E^{-3}	7.15 E^{-5}	14.07	0.09	-0.01	0.99997
	C_2H_6	-3816.75	56.20	1.28	-0.03	9.90 E^{-4}	-1.22 E^{-5}	15.64	-0.15	-3.01 E^{-3}	0.99994

Table S4. Comparison about the IAST selectivity of some top-ranking C_2H_6-selective MOFs reported previously at 100 kPa.

Adsorbents	C_2H_6/C_2H_4 (50:50,v/v)	C_2H_2/C_2H_4 (1:99,v/v)	Ref.	Adsorbents	C_2H_6/C_2H_4 (50:50,v/v)	C_2H_2/C_2H_4 (1:99,v/v)	Ref.
Azole-Th-1	1.46	1.09	1	**Zn-ad-int**	2.4	1.61	2
NPU-1	1.32	1.39	3	**NPU-3**	1.52	1.32	3
MOF-525	1.25	1.48	4	**MOF-525(Co)**	1.10	1.92	4
UPC-612	1.47	1.07	4	**UPC-613**	1.47	1.37	4
Zn-atz-oba	1.27	1.42	5	**TJT-100**	1.2	1.8	6
UiO-67-(NH_2) (296K)	1.70	2.1	7	**UPC-66-a (293K)**	1.65	1.05	8
CuTiF6-TPPY	2.12	5.03	9	**MOF-808-Bzz**	1.90	3.15	10
BUT-150	1.15	1.82	11	**BUT-151**	1.26	1.61	11
MOF-808	1.10	3.65	This work	**MOF-808-1Fc**	1.09	2.46	This work
MOF-808-3Fc	1.21	2.34	This work	**MOF-808-6Fc**	1.56	3.54	This work

Table S5. The calculated heat of adsorption (Qst) on samples.

Samples	C_2H_2 (kJ·mol^{-1})	C_2H_4 (kJ·mol^{-1})	C_2H_6 (kJ·mol^{-1})
MOF-808	36.16	20.37	20.69
MOF-808-1Fc	35.07	26.08	27.50
MOF-808-3Fc	30.35	26.99	28.76
MOF-808-6Fc	32.36	27.38	31.73

Table S6. Summarized production cost of MOF-808-6Fc.

Raw materials	Price (CNY/t)
1,3,5-benzenetricarboxylic acid （98%）	389800
$ZrOCl_2·8H_2O$ （99%）	298000
Formic acid	30000
Ferrocene carboxylic acid （98%）	4358000
DMF （99.5%）	42000
Acetone	63300

References

[1] Z. Xu, X. Xiong, J. Xiong, R. Krishna, L. Li, Y. Fan, F. Luo, B. Chen, *Nat Commun.* **2020,** *11*, 3163.

[2] Q. Ding, Z. Zhang, Y. Liu, K. Chai, R. Krishna, S. Zhang, *Angew Chem Int Ed.* **2022,** *61*, e202208134.

[3] B. Zhu, J. W. Cao, S. Mukherjee, T. Pham, T. Zhang, T. Wang, X. Jiang, K. A. Forrest, M. J. Zaworotko, K. J. Chen, *J Am Chem Soc.* **2021,** *143*, 1485-1492.

[4] Y. Wang, C. Hao, W. Fan, M. Fu, X. Wang, Z. Wang, L. Zhu, Y. Li, X. Lu, F. Dai, Z. Kang, R. Wang, W. Guo, S. Hu, D. Sun, *Angew Chem Int Ed.* **2021,** *60*, 11350-11358.

[5] J. W. Cao, S. Mukherjee, T. Pham, Y. Wang, T. Wang, T. Zhang, X. Jiang, H. J. Tang, K. A. Forrest, B. Space, M. J. Zaworotko, K. J. Chen, *Nat Commun.* **2021,** *12*, 6507.

[6] H. G. Hao, Y. F. Zhao, D. M. Chen, J. M. Yu, K. Tan, S. Ma, Y. Chabal, Z. M. Zhang, J. M. Dou, Z. H. Xiao, G. Day, H. C. Zhou, T. B. Lu, *Angew Chem Int Ed.* **2018,** *57*, 16067-16071.

[7] X. W. Gu, J. X. Wang, E. Wu, H. Wu, W. Zhou, G. Qian, B. Chen, B. Li, *J Am Chem Soc.* **2022,** *144*, 2614-2623.

[8] Y. Wang, M. Fu, S. Zhou, H. Liu, X. Wang, W. Fan, Z. Liu, Z. Wang, D. Li, H. Hao, X. Lu, S. Hu, D. Sun, *Chem.* **2022,** *8*, 3263-3274.

[9] P. Zhang, Y. Zhong, Y. Zhang, Z. Zhu, Y. Liu, Y. Su, J. Chen, S. Chen, Z. Zeng, H. Xing, S. Deng, J. Wang, *Sci Adv*. **2022**, 8, eabn9231.

[10] C. Song, F. Zheng, Y. Liu, Q. Yang, Z. Zhang, Q. Ren, Z. Bao, *Angew Chem Int.* **2023,** *62*, e202313855.

[11] H.-T. Wang, Q. Chen, X. Zhang, Y.-L. Zhao, M.-M. Xu, R.-B. Lin, H. Huang, L.-H. Xie, J.-R. Li, *Journal of Materials Chemistry A.* **2022,** *10*, 12497-12502.